High-Purity Semi-Insulating 4H-SiC Grown by the Seeded-Sublimation Method

J.R. JENNY, ST.G. MÜLLER, A. POWELL, V.F. TSVETKOV, H.M. HOBGOOD, R.C. GLASS, and C.H. CARTER, Jr.

Cree Inc., Durham, NC 27703

The growth of high-purity, semi-insulating (HPSI) 4H-SiC crystals has been achieved using the seeded-sublimation growth technique. These semi-insulating (SI) crystals (2-inch diameter) were produced without the intentional introduction of elemental deep-level dopants, such as vanadium, and wafers cut from these crystals possess room-temperature resistivities greater than 10^9 Ωcm. Based upon temperature-dependent resistivity measurements, the SI behavior is characterized by several activation energies ranging from 0.9–1.5 eV. Secondary ion mass spectroscopy (SIMS) and electron paramagnetic resonance (EPR) data suggest that the SI behavior originates from deep levels associated with intrinsic point defects. Typical micropipe densities for wafers were between 30 cm^{-2} and 150 cm^{-2}. The room-temperature thermal conductivity of this material is near the theoretical maximum of 5 W/mK for 4H-SiC, making these wafers suitable for high-power microwave applications.

Key words: High-purity semi-insulating, HPSI, 4H-SiC, seeded sublimation, physical vapor transport, SIMS, EPR, resistivity, thermal conductivity

INTRODUCTION

The future of wireless communications, including wide-band internet access and video-on-demand is heavily dependent upon the development of a new generation of semiconducting materials that have properties to facilitate highly linear, high-power field-effect transistors. Due to its unique materials properties,[1] silicon carbide has great potential to make significant inroads in the wireless arena. To take advantage of the unique properties of SiC for microwave devices, semi-insulating (SI) substrates are required. The principal mechanism for the formation of SI semiconductors is through the use of deep-level dopants, which pin the Fermi level to near the middle of the bandgap. After decades of research in SiC, the only viable deep-level dopant that has emerged is vanadium, acting both as a deep-level donor[2,3] and a deep-level acceptor.[4] Although vanadium is used to grow the majority of commercially available SI SiC substrates, recent reports[5] suggest that vanadium may not be the optimum deep-level dopant for SiC. Analogous to the GaAs developments of the early 80s where Cr was deemed an unsuitable deep-level dopant,[6] and the intrinsic EL2 defect arose a suitable alternative, we have investigated the use of intrinsic SiC defects to pin the Fermi level deep enough in the bandgap to produce SI 4H-SiC wafers. In this work, we present the characterization of these substrates using a range of techniques, including secondary ion mass spectroscopy (SIMS), resistivity mapping, electron paramagnetic resonance (EPR), temperature-dependent resistivity measurements, flash-method thermal conductivity, and scanning thermal microscopy.

(Received September 14, 2001; accepted February 5, 2002)

EXPERIMENTAL DETAILS

Wafers

The 4H-SiC single crystals are grown using physical vapor transport via seeded sublimation. This technique has been reviewed[7] and is currently the preferred method for the bulk growth of monocrystalline SiC. The SI 4H-SiC crystals were grown without the intentional introduction of elemental deep-level impurities. Typical micropipe densities of wafers used in this study were approximately 50 cm^{-2}.

Electron-Paramagnetic Resonance

The EPR spectra were recorded with a Bruker EMX spectrometer equipped with an Oxford ESR

900 continuous flow cryostat. All measurements were taken at 50 K and in X-band (~9.75 GHz), with samples ($10 \times 2.75 \times 0.4$ mm^3) cut from c-axis wafers.

Resistivity Mapping

To map the resistivity of an HPSI substrate, a technique was employed that took advantage of the physical relationship of a homogeneous semiconductor between the dielectric relaxation time, τ, and the resistivity, ρ: $\tau = \varepsilon \cdot \varepsilon_o \cdot \rho$ (ε: dielectric constant and ε_o: permittivity of the vacuum). The system (measurement range: 10^6–10^{12} Ωcm) uses a pulse technique to measure τ directly from the response as a function of time and allows for high lateral resolution.[8]

Temperature-Dependent Resistivity

The temperature-dependent resistivity data was collected on a custom-built, high-temperature (up to 1300 K) Hall-effect system. The system is comprised principally of instrumentation to yield the highest-possible impedance system while maintaining complete automation.

Thermal Conductivity

Thermal conductivity was measured using the flash method that has been well documented for the study of SiC.[9,10] Additionally, scanning thermal microscopy[11] was employed to determine the cross-wafer variation in thermal conductivity.

RESULTS

Material Purity

Elemental Analysis

Table I is a listing of the impurities that were examined by SIMS and their respective concentrations for representative HPSI material. This survey encompassed the bulk of the first-row transition element series as well as other common impurities in SiC. The only elements observed using SIMS in HPSI material are nitrogen (typically ~5E16 cm^{-3}) and boron (typically ~1.5E16 cm^{-3}), while the concentrations of all other elements were below the SIMS detection limits or below the instrument background (as in the case of oxygen). The actual detection limit for oxygen is below the level indicated, but system oxygen was not completely removed, resulting in the stated concentration.

Table I. The SIMS Analysis of 4H-SiC HPSI Material (the Only Elements Detected Are the Shallow Level Impurities Nitrogen and Boron)

Element	Concentration (cm^{-3})
B	1.50E + 16
N	5.00E + 16
Na,* A1*	<5.00E + 13
Ti*	1.00E + 14
V,* Cr*	5.00E + 13
Fe,* P*	2.00E + 14
Ni,* F*	5.00E + 14
Cu*	3.00E + 14
O**	4.00E + 16
C,* Cl*	1.40E + 15
As*	7.00E + 14

*Value at SIMS detection limit.
**Value at instrument background limit.

Electrical Characterization

Resistivity Uniformity

A plot of resistivity over the area of a 2-inch-diameter HPSI wafer is shown in Fig. 1. This room-temperature map indicates clearly that the material is SI. The lowest resistivity values were 2×10^9 Ωcm, while most of the wafer exhibited resistivities greater than the upper limit of the technique ($>3 \times 10^{11}$ Ωcm). The slight resistivity variation across the wafer can be explained by Fermi level variations due to the various electrical levels present in the wafer. Because both boron and nitrogen are shallow impurities in SiC, and they are the only impurities detected by SIMS in this HPSI material, the question of why this material is SI arises.

Electrical Activation Energy

To more fully understand the resistivity results, temperature-dependent resistivity measurements were undertaken to determine the activation energy of the defects responsible for the SI character (Fig. 2). An examination of the resistivity vs. temperature for different samples, from different SI crystals, reveals multiple activation energies: 0.9, 1.1, 1.2, 1.35, and 1.5 eV. As a result, not one, but several defects are responsible for the SI character in this HPSI material. While the activation energies are only separated by 0.1–0.2 eV, they are believed to be distinct levels based upon the measurement of a statistically significant number of samples. More accurate analysis based upon the

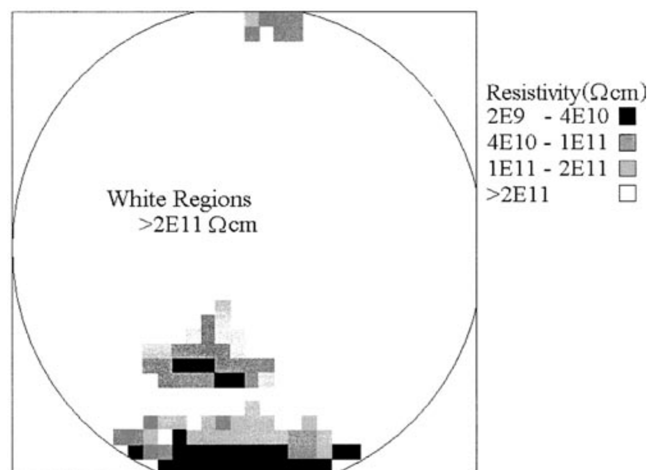

Fig. 1. High-resolution resistivity map of a 50-mm-diameter 4H-SiC HPSI wafer. The whole wafer is SI, while more than 80% of the wafer area has a resistivity $>3 \times 10^{11}$ Ωcm.

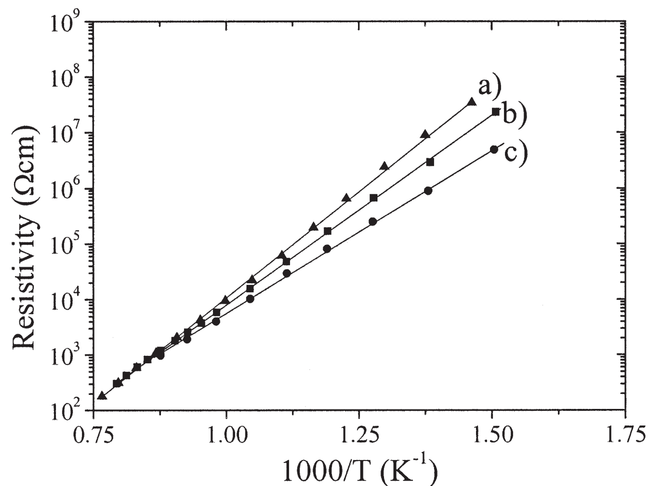

Fig. 2. Resistivity vs. temperature for three 4H-SiC HPSI samples whose activation energies are (a) 1.53 eV, (b) 1.33 eV, and (c) 1.19 eV.

temperature dependence of the carrier concentration was not possible due to the low Hall mobilities found in the samples. This lower mobility could result from (a) mixed-carrier conduction[12] (for the deepest levels) or (b) a variation in the Fermi level position across the individual van der Pauw samples.[13] Additionally, while complexes with boron and nitrogen cannot be ruled out, this resistivity data coupled with the SIMS results indicates that the source of the deep levels is likely to be intrinsic in nature.

Defect Structural Characterization

Electron Paramagnetic Resonance

Figure 3 is an EPR spectrum of a sample exhibiting an activation energy of 1.5 eV. The large sharp peak with two hyperfine doublets is the main feature in this spectrum. It has been previously identified as a carbon vacancy.[14] Photo-EPR measurements by another group on similar material place the activation energy of this carbon vacancy defect at 0.9–1.2 eV above the valence band.[15] The fact that the defect is present in SI material (and not readily visible in p- or n-type material suggests that it is electrically active and is responsible for at least one of the defects observed in the temperature-dependent resistivity measurements.

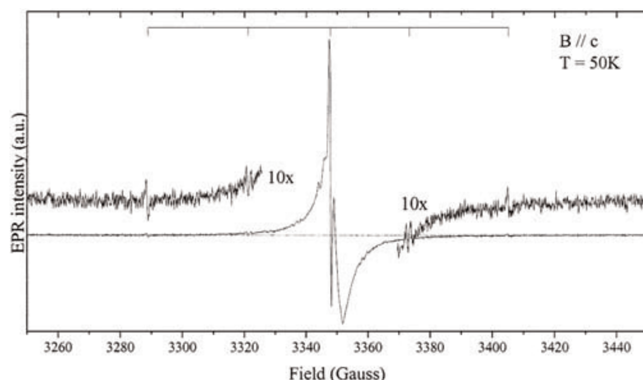

Fig. 3. The EPR spectrum of a 4H-SiC HPSI sample whose Fermi level was pinned to the 1.5-eV level and exhibits the carbon vacancy.

Materials Characterization

Thermal Conductivity

To more fully understand this extremely important characteristic of our HPSI material, we have employed two types of thermal conductivity measurements (the flash method and scanning thermal microscopy). Data from the flash-method measurements are shown in Fig. 4. The solid curves represent calculations based upon the theory developed by Callaway[16] for thermal conductivity, using only U and N processes. The flash-method measurements (indicated by the various symbols) reveal that the room-temperature thermal conductivity is 4.9 W/cmK, very near the theoretical limit calculated for undoped 4H-SiC. Additional measurements using scanning thermal microscopy showed that the thermal conductivity was constant across the wafer. This uniform, extremely high, thermal conductivity is essential for the creation of the next generation of electronic devices envisioned for SiC.

CONCLUSIONS

HPSI 4H-SiC has been grown by the seeded-sublimation technique without the intentional introduction of deep-level defects. Conclusions drawn from chemical and electrical analyses of this material are as follows.

- High-lateral resolution resistivity mapping has shown that the wafers are SI across the full 2 in. wafer diameter.
- An analysis of temperature-dependent resistivity measurements shows the SI character is controlled by the presence of multiple deep levels.
- These deep levels are attributed to intrinsic point defects because SIMS on this material reveals the presence of only boron and nitrogen, which form shallow electronic levels in SiC.
- EPR measurements performed on these samples suggest that one of these defects is the carbon vacancy.

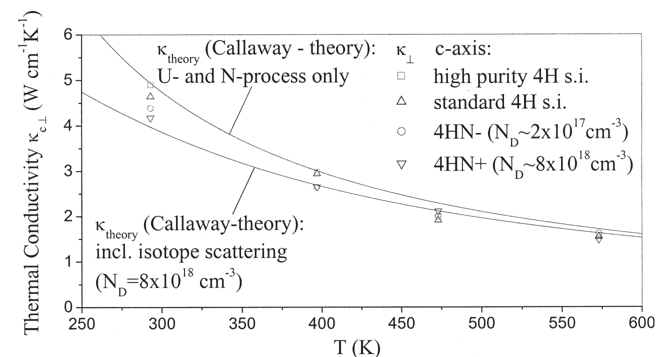

Fig. 4. Flash-method thermal conductivity for heat flow perpendicular to the c axis of the samples. The thermal conductivity for HPSI samples is at the theoretical limit for 4H-SiC (based upon Callaway).

Taken together, all of these analyses reveal that the formation of HPSI 4H-SiC can be accomplished using seeded-sublimation growth. This SI character coupled with the high thermal conductivity of HPSI material makes it potentially an excellent substrate for SiC metal-semiconductor field-effect transistor and monolithic-microwave integrated circuit applications.

ACKNOWLEDGEMENTS

This work was supported in part by the Air Force Research Laboratories, the Office of Naval Research, and BMDO.

REFERENCES

1. R.F. Davis, G. Kelner, M. Shur, J.W. Palmour, and J.A. Edmond, *IEEE Proc.* 79, 677 (1991).
2. K. Maier, H.D. Muller, and J. Schneider, *Mater. Sci. Forum* 83–87, 1184 (1992).
3. J.R. Jenny, M. Skowronski, W.C. Mitchel, H.M. Hobgood, R.C. Glass, G. Augustine, and R.H. Hopkins, *J. Appl. Phys.* 78, 3839 (1995).
4. J.R. Jenny, M. Skowronski, W.C. Mitchel, H.M. Hobgood, R.C. Glass, G. Augustine, and R.H. Hopkins, *Appl. Phys. Lett.* 68, 1963 (1996).
5. E. Morvan, O. Norblanc, C. Dua, and C. Brylinski, *Mater. Sci. Forum* 353–356, 669 (2001).
6. C. Kocot and C.A. Stolte, *IEEE Trans. Microwave Theory Tech.* MTT-30, 963 (1982).
7. S.G. Müller, R.C. Glass, H.M. Hobgood, V.F. Tsvetkov, M. Brady, D. Henshall, J.R. Jenny, D. Malta, and C.H. Carter Jr., *J. Cryst. Growth* 211, 352 (2000).
8. R. Stibal, J. Windscreif, and W. Jantz, *Semicond. Sci. Technol.* 6, 995 (1991).
9. W.J. Parker, R.J. Jenkins, C.P. Butler, and G.L. Abbott, *J. Appl. Phys.* 32, 1679 (1961).
10. R.C. Heckman, *J. Appl. Phys.* 44, 1455 (1973).
11. D.I. Florescu, F.H. Pollak, G.R. Brandes, B.E. Landini, and A.D. Salant, *Mater. Res. Soc. Proc.* 680E, E2.4.1-6 (2001).
12. D.C. Look, *Semicond. Semimet.* 19, 75 (1983).
13. J. Vaitkus, J. Storasta, R. Kiliulis, V. Rinkevicius, S. Slenys, S. Smetona, S. Meskinis, K.M. Smith, and V. O'Shea, *Nucl. Inst. Meth. Phys. Res. A* 394, 94 (1997).
14. N.T. Son, P.N. Hai, and E. Jansen, *Phys. Rev. B* 63, 201201 (2001).
15. M.E. Zvanut and V.V. Konovalov, *Appl. Phys. Lett.* 80, 410 (2002).
16. S.G. Müller, R. Eckstein, J. Fricke, D. Hofmann, R. Horr, H. Mehling, and O. Nilsson, *Mater. Sci. Forum* 264–268, 623 (1998).